NON-INTRUSIVE CURRENT-BASED FAULT DETECTION OF ELECTRO-MECHANICAL ACTUATORS WITH BRUSHED DC MOTORS

Ondřej Hanuš, Radislav Smid

*Czech Technical University in Prague, Faculty of Electrical Engineering, Department of Measurement, Technicka 2,
166 27 Prague, Czech Republic (✉ hanuson1@fel.cvut.cz, +420 22435 2346, smid@fel.cvut.cz)*

Abstract

This paper proposes data-based fault detection methods for an electromechanical actuator (EMA) with
a brushed DC motor. The jam and winding short faults are considered in the study as the most prominent
EMA faults. The fault detection is based on evaluating the properties of the motor current, considering the
basic electromechanical parameters of EMAs. The main advantages are a non-intrusive approach utilising
a commonly accessible motor current measurement, simple configurability, and the ability to detect faults
under varying operation modes of EMA, including changes of speed, load, or movement profiles. The
proposed methods have been evaluated with a custom testing system, and the results have proven the
performance of the proposed approach to detect faults under varying operating conditions in industrial
applications.

Keywords: Electro-mechanical Actuator (EMA), Fault Detection and Diagnostics (FDD), jam, winding
short.

1. Introduction

Electro-mechanical actuators (EMAs) are among the most widespread types of linear actua-
tors. They are used in many industries, including automotive, mechanical engineering, robotics
or aerospace. The main advantages of these actuators are their simplicity, reliability, easy con-
trol, compact size, and high power density. Undetected failures and degradations of EMAs can
lead to an increase in repair and maintenance costs and could be dangerous, especially in safety-
critical applications. To prevent failures, embedded fault detection systems for EMAs are required,
consequently there is a need for low-complexity unsupervised fault detection methods.

In recent decades, considerable efforts have been made to develop diagnostic methods for
EMAs. These methods can be divided into two categories: model-based and data-based ap-
proaches. Model-based approaches require a mathematical model that will correspond as closely
as possible to the behaviour of an actual device. The advantage is that degradations can be tracked

based on changes in model parameters. The disadvantage is that the models tend to be too complex and need to be thoroughly validated [1].

In [2], a model-based fault detection approach uses the evaluation of discrepancy between the commanded position and the actual position or between positions of two parts of the actuator. [3] demonstrates a model-based *prognostic health management* (PHM) algorithm for identifying the mechanical transmission backlash using the limit cycle oscillations in the EMAs position values.

In contrast to model-based approaches, data-based approaches use various patterns or signatures evaluated in monitored signals [1].

In [4] the researchers present the detection of a return channel jam, spalling and sensor faults using an artificial neural network trained by temperature and vibration data. In [1], the fault detection approach is based on vibration and motor current signatures in the frequency domain synchronous with the motor position. The paper [5] presents the method based on signal parameters such as steady value, overshoot, settling time, or the presence of unexpected peaks from the electric current and position measurement to detect lack of lubrication, spalling and backlash. The work [6] utilises the *Computed Order Technique* (COT) to transform transient vibrations into ordered vibrations; their frequencies are used to detect a partial jam and spall in the EMA ballscrew mechanism. The research presented in [7] describes a health monitoring approach based on statistical process monitoring to detect loss of control and an actuator jam. The researchers in [8] describe how to detect faults using vibration data measured under different working conditions by semi-supervised learning and neural networks.

Fault detection in EMAs is difficult due to their dynamic behaviour during operation (frequent changes in speed and direction). Some methods compensate for rotational speed dynamics, such as order tracking [6] or Vold–Kalman filtering [9]; however, implementing these methods is costly due to computational complexity or necessary installation of additional sensors.

This paper proposes a novel non-intrusive approach for jam and winding short fault detection of an electromechanical actuator with a permanent magnet DC brush motor. The proposed methods depend on a single quantity measurement – the electrical current intensity. They are designed to deal with the dynamic behaviour of EMAs doing so without any other additional sensors or sources of information.

2. Detection of EMA faults

2.1. Signal description

The proposed fault detection methods are based on evaluating the features of electric current specific for an EMA with a brushed DC motor. Both methods process the absolute values of the measured current, and therefore the direction of movement is not apparent from the collected data. The typical current waveform, influenced by mechanical and electrical properties of the actuator, can be seen in Fig. 1.

A PWM control of motor speed causes the high-frequency component in the raw current. The current switching is driven by a PWM signal, defined by the frequency f_P and duty cycle D expressed in percentage. The effect of switching is more noticeable at lower values of D and completely disappears at $D = 100\%$. It can be seen in Fig. 1 during the motor run-up. The D is about 50% at the beginning to decrease the inrush current. It increases up to 100% with the rise of the motor speed, and the effect of switching disappears.

The low-frequency oscillations in the waveform are caused by commutation spikes which occur when the brush breaks the contact with the commutator sector connected to the energized
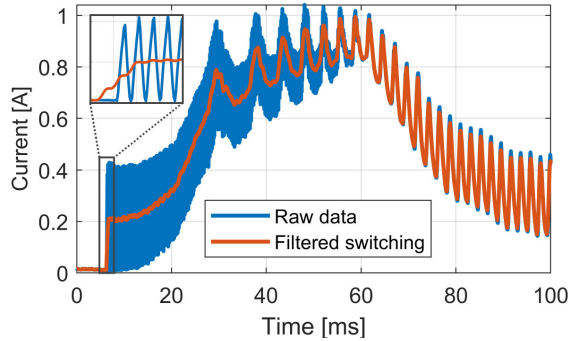
Fig. 1. Electric current during the controlled run-up of the EMA
with a zoomed detail of the switching effect.

winding. Figure 1 shows the filtered signal where the switching effect was suppressed while commutation spikes are still visible. Commutation spikes are directly related to motor rotation, and therefore this information is essential for fault detection.

2.2. Jam detection

The jam of an EMA can be caused by many factors such as excessive overload or wear, insufficient lubrication of the moving parts, mechanical damage or thermal stress. As a result, the jammed actuator cannot move, which causes further overloading and, possibly, some extent of the damage. The overcurrent protection might be used as a countermeasure against the jam. However, for low duty cycles of PWM, the actual current can be lower than the current for maximum load, and the protection fails. This problem is solved by the proposed algorithm depicted in Fig. 2.
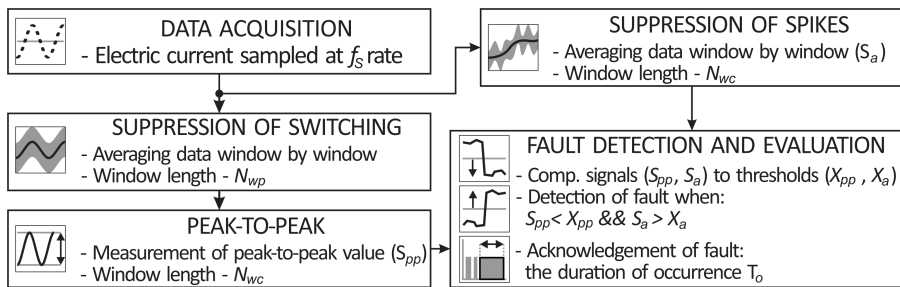

Fig. 2. Block diagram of the jam detection algorithm.

Raw sampled data from the block "Data Acquisition" are first filtered. The block, called "Suppression of Switching", suppresses high-frequency components caused by the PWM motor control. The output from this block still contains commutation spikes that provide information about the motor's movement. The second filtering block, called "Suppression of Spikes", aims to eliminate both high-frequency PWM switching components and low-frequency commutator oscillations. The output represents the averaged motor current over time and gives the information on whether the motor is under load.

www.czasopisma.pan.pl   PAN   www.journals.pan.pl
POLSKA AKADEMIA NAUK

O. Hanuš, R. Smid: NON-INTRUSIVE CURRENT-BASED FAULT DETECTION OF ELECTRO-MECHANICAL ACTUATORS...

Standard digital filters (FIR/IIR) can be computationally intensive; in this paper, a different approach was chosen. The filtration was done by averaging data with different windows length without overlap. This approach worsen resolution in time but reduces computational complexity.

The length of the window for suppression of switching is based on the sampling frequency f_S and PWM switching frequency f_P as

$$N_{wP} = a \cdot \frac{f_S}{f_P},$$ (1)

where N_{wP} is the length of the window, a is the factor that extends averaging over multiple periods, and the f_P is the lowest PWM switching frequency.

The suppression of commutation spikes is based on the EMA's lowest speed of motion. The length of the window for suppression of commutation spikes is calculated as

$$N_{wc} = f_S \cdot T_{\max},$$ (2)

where N_{wc} is the window's length, f_S is the sampling frequency, and $T_{\max}$ is the longest time of a commutation spike measured during the slowest possible movement of the EMA without load.

The filtered data with the commutation oscillations are used to detect movement, while the filtered data without oscillations are related to load. The proposed algorithm measures a peak-to-peak (pp) value of the signal with commutations for motion detection. This value is calculated using the window with a length equal to N_{wc}.

The last part of the algorithm are fault detection and evaluation that process peak-to-peak and averaged signals. The presence of significant values of the peak-to-peak signal represents the rotation of the motor. In contrast, low values mean that the motor is not moving. The X_{pp} threshold is used to distinguish between these two states. In the case when the motor is not moving, it can be either jammed or stopped. The averaged current is used to assess these situations by a comparison with the X_a threshold. If the average current is above the X_a and at the same time the peak-to-peak signal is below X_{pp}, a fault is detected. The peak-to-peak signal and averaged current values can vary substantially during operation, mainly due to the change in load, movement speed, and operating regimes. Thresholds must be set accordingly to cover all possible states. They can be determined from the measurements on the EMA without any load at the lowest possible speed. Values of the peak-to-peak signal and averaged current are minimal in this condition compared to all possible states during the nominal operation of the EMA. The proposed method uses thresholds that are established as 50% of these minimal measured values to ensure acceptable margins.

When a fault is detected, it is acknowledged by the duration of the occurrence. It is assumed that the jammed actuator remains in this state for some time. The acknowledgement procedure prevents incorrect identification of faults that may occur during the slow movement of the actuator. A necessary condition is that evaluation time T_o is always higher than $T_{\max}$.

2.3. Winding short detection

Electrical faults in motors are among the most common faults in electromechanical actuators. Typical faults include winding shorts and open winding [4]. The proposed method focuses on detecting rotor winding shorts that arise in the case of an insulation failure between coil turns. The most critical are shorts between the individual coils of the rotor [10]. They are usually caused by the degradation of the insulation due to thermal effects, contamination or centrifugal force (for a detailed overview, see [11]). The defect of shorted winding causes a reduction in torque and changes in resistivity, inductance, which usually do not lead to a complete loss of EMA

functioning. The extent of motor's electrical imbalances depends on the number of shorted turns and arrangment of the winding [10].

During the operation of the brushed DC motor, the damaged winding is energised twice in one revolution, every time with opposite polarity. Thus, the increased current's electrical imbalance should be noticeable at twice the motor's speed. The motor current signal analysis shows that the commutation peaks' dominant frequency is a multiple of the motor's speed. The relation between the motor speed expressed as motor frequency f_M, fundamental commutation frequency f_C and frequency of winding short fault f_{ws} can be described by the following equations:

$$f_C = N_C \cdot f_M \,, \tag{3}$$

$$f_{ws} = 2 \cdot \frac{f_C}{N_C} = 2 \cdot f_M \,, \tag{4}$$

where N_C is the number of commutator segments resulting from the commutator arrangement.

The algorithm for winding short detection is depicted in Fig. 3; it comprises four parts; data sampling, data selection, spectrum analysis and fault evaluation.
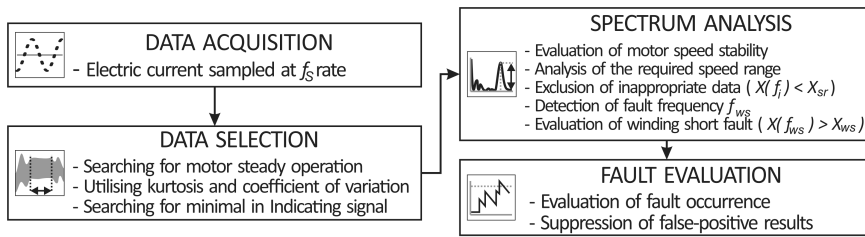

Fig. 3. Block diagram of the winding short detection algorithm.

The sampled data are processed in windows of the length based on the system's parameters, such as the maximal speed of rotation and number of measured rotations. The measured time interval should be short of catching the motor's steady operation but with reasonable resolution in the frequency spectrum. Also, it should be long enough to capture periodicity in the measured signal. It is therefore preferable to perform the detection at higher motor speeds. The measured time interval is established for 50% of motor's speed as

$$T_d = r \cdot \frac{60}{v_{\max} \cdot 0.5} \,, \tag{5}$$

where r is the number of revolutions required for analysis and $v_{\max}$ is the maximal rotation speed of the tested motor in RPM. The resolution in the frequency spectrum is directly related to the measured time interval, and it is described as

$$f_\Delta = f_S / N_W = f_S / (f_S \cdot T_d) = 1/T_d \,, \tag{6}$$

where f_S is the sampling frequency and N_W is the length of the window. Ten per cent or lower values of the lowest frequency of interest should be sufficient resolution for spectrum analysis.

Electromechanical actuators can be controlled up to a specific position, to required motion profiles or other desired parameters based on the particular case of use. Rapid control actions of the controller cause dynamic changes in EMA's speed and direction of movement that are also reflected in the measured current. The proposed method brings a novel approach to dealing with the dynamic changes of EMA behaviour during control; fault detection is provided in short time

509

www.czasopisma.pan.pl   PAN   www.journals.pan.pl
POLSKA AKADEMIA NAUK

O. Hanuš, R. Smid: NON-INTRUSIVE CURRENT-BASED FAULT DETECTION OF ELECTRO-MECHANICAL ACTUATORS . . .

segments where the signal is near a steady state. Kurtosis is used to assess the steady state; outliers primarily determine its value [12]. It reaches highs when the signal is not regular, and conversely, lows indicate a steady state. The motor current signal can also vary with the speed and load; the coefficient of variation is used to compensate for these fluctuations. Multiplying these parameters produces an indicating signal that is calculated over the T_d period as

$$
I_s = k \cdot \hat{c_v} = \frac{\frac{1}{n} \sum_{i=1}^{n} (x_i - \overline{x})^4}{\left(\frac{1}{n} \sum_{i=1}^{n} (x_i - \overline{x})^2 \right)^2} \cdot \frac{s}{\overline{x}} ,
\tag{7}
$$

where k is kurtosis, $\hat{c_v}$ is the coefficient of variation, n is the number of samples, $\overline{x}$ is mean and s is standard deviation. The minimum in every ten samples of the indicating signal is used to select data that are suitable for subsequent analysis.

The detection of a winding short fault is based on the *Motor Current Signature Analysis* (MCSA) [13, 14] using amplitude spectrum. Spectrum analysis is performed only on the block of data that the data selection procedure provided. The main goal of this analysis is to identify f_C and then search winding short fault represented by f_{ws}. The spectrum is gradually analysed in different ranges depending on the maximum engine speed. The border frequencies of desired range can be expressed by the f_C as

$$
f_C = D_M \cdot N_C \cdot \frac{v_{\max}}{60 \cdot 100} ,
\tag{8}
$$

where D_M is the desired percentage of maximum motor speed.

The first step of the algorithm is to find a significant peak (f_i). The spectrum is analysed at a narrower frequency range corresponding to 50 to 100% of maximum motor speed at first. Only the fundamental frequency of f_C or its second harmonics f_{2C} should be present within this range. When no significant frequencies are found, the range is extended to 25 to 125%, and the process is repeated. This wider range is beneficial in the cases when the motor is rotating faster than maximal RPM given by the manufacturer (the actual f_C is higher than maximal expected f_C, (see (8)) or slower than 50% when the peak of second harmonic is insignificant. However, the analysis in the narrower frequency range must always be performed first to prevent confusion of higher harmonics of f_C with the fundamental in the broader range. The required range of the spectrum is always searched in descending order until a peak is found. If no significant peaks are found, the tested block of data is discarded. Otherwise, the amplitude of the found peak is compared to the mean value in this range. The low ratio between them indicates the changing motor speed (smeared peak), and the data block is also excluded from the analysis. The peak with a high ratio is further investigated. The threshold for this step (X_{sr}) can be determined based on measurements conducted during nominal operation at the 25% of speed and without load, because the amplitude of f_C reaches the lowest values acceptable for analysis. It might be established as a multiple of mean value that is still lower than the amplitude of f_C at this speed.

The next step is to verify whether the frequency of the investigated peak (f_i) is the fundamental commutation frequency (f_C). The amplitudes at f_i and $f_i/2$ are compared. If the amplitude of $f_i/2$ is higher than amplitude at f_i, it means that $f_i/2$ is fundamental commutation frequency (f_C). Otherwise, f_i is the fundamental commutation frequency. The found f_C is used for fault detection. The detection is based on searching for the significant amplitude at twice f_M (see (4)). The height of the peak f_{ws} reflects the extent of the fault. The X_{ws} threshold defining the fault can be established by comparing the amplitudes of f_{ws} and f_C.

Fault evaluation is used to suppress unwanted false-positive results by the failure/pass counting. Identified failures increase the error value faster than passes that decrease the error value. When the error value exceeds the preset threshold, the motor's fault is indicated.

2.4. Fault detection concept

The proposed approach utilizes the non-intrusive concept that is depicted in Fig. 4. The fault detection procedure uses only current measurement, either using current clamps on the supply cables or output from power drive electronics that allows current sensing. If a fault is detected, a warning signal is sent to either deactivate the actuator or take the necessary action to prevent damage. The fault detection procedure does not interfere with the actuator in any way and therefore can be implemented as part of the control electronics.
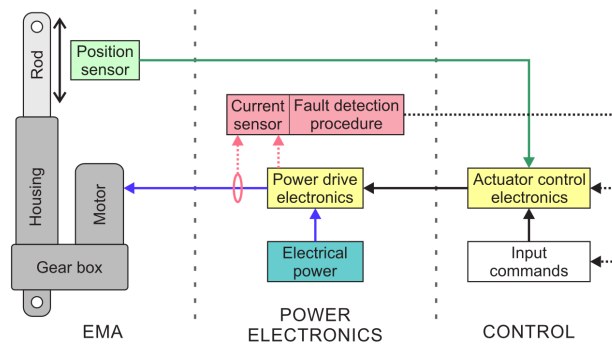
Fig. 4. Block diagram of the fault detection concept.

3. Testing system

3.1. Block diagram

For validation of the proposed methods, a custom EMA testing system was developed. The fundamental parts of the system are depicted in Fig. 5.
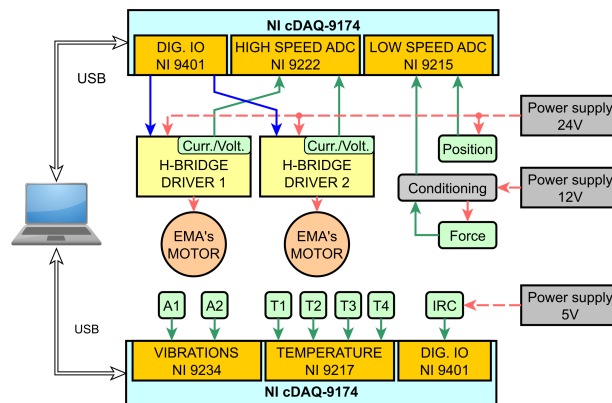

Fig. 5. Block diagram of the testing system.

The system is composed of a PC connected over the USB to two NI cDAQ chassis. The main chassis (top branch of the diagram) is responsible for actuators control and basic data acquisition. The control of actuator motors is achieved by an NI 9401 module that generates PWM pulses for two integrated H-bridge circuits. The main chassis includes two modules for data acquisition; high-speed acquisition of current and voltage and low-speed acquisition of position and force. The position and force sensor data are used as feedback for controlling movement and load during testing.

The secondary chassis (bottom branch of the diagram in Fig. 5) is used for additional measurements. The properties of all depicted sensors are summarised in Table 1.

Table 1. Parameters of used sensors.

Measurement	Range	Acq. sampling rate (during experiments / max. possible)
Force	±500 N	1 kHz / 100 kHz
Position	225 mm	1 kHz / 100 kHz
Motor current	15 A	200 kHz / 500 kHz
Motor voltage	±32 V	200 kHz / 500 kHz
Temperature	−30/200°C	1 Hz / 100 Hz
Vibrations	Peak 60 g, 0.3–6000 Hz	51.2 kHz / 51.2 kHz
Motor rotation	200 CRP	Given by rotation speed (up to 20 kHz)

A Honeywell Load Cell 151 is used as a force sensor. It is an S-beam tension and compression sensor that is, besides the data acquisition, used in a load control loop. Also, data from the sensor are utilised in a safety feature that protects the system from overloading. The position is measured with a Honeywell SPS-L225-HALS magnetoresistive linear sensor. This sensor allows controlling the movement of the tested actuator on predefined paths. The system enables motor current measurement with a current clamp or a current sensing pin, part of the H-bridge driver. The frequency range of the Fluke i30s current clamp is from DC to 100 kHz, allowing the analysis of artefacts caused by PWM switching. In contrast, the H-bridge current sensing significantly suppresses PWM switching artefacts, which may be beneficial for some types of analysis that would otherwise require low-pass filtering. A voltage is acquired utilising the voltage divider placed directly next to the motor supply cables. The temperatures are measured with four miniature Pt100 sensors (indicated in diagram as T1, T2, T3 and T4), whose positions can be changed depending on the specific demands of an experiment. The typical placement of temperature sensors is at the motor, gearbox, rod housing and frame of the testing system to measure ambient temperature. The system offers two measurements of vibrations using two Bruel&Kjaer 4507-B-004 accelerometers (indicated in diagram as A1 and A2), usually placed at the motor and the gearbox. The rotation of the tested motor is measured with an 5421-ep111 optical encoder.

The system allows conducting experiments with one or two EMAs, depending on the requirements of tests. Two different EMAs with similar parameters were used during experiments. The DSZY1 actuator is manufactured by the Drive-Systems Europe Ltd and TA 2 actuator by Timotion. The detailed picture with a description of actuators is in Fig. 6. Both EMAs consist of a brushed DC motor, a speed reducer gearbox and a housing with a rod that uses a screw and nut to transform rotary to linear motion. The parameters of tested actuators are shown in Table 2.
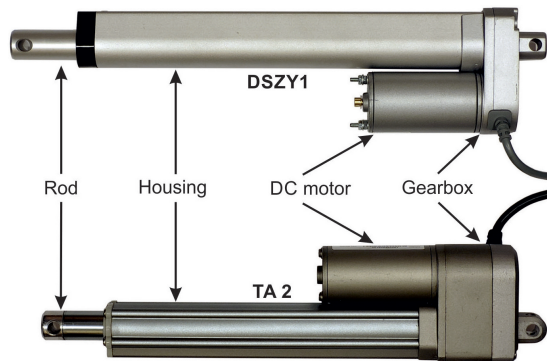
Fig. 6. DSZY1 and TA 2 actuators used during experiments.

Table 2. Parameters of the tested EMAs.

Parameter	DSZY1	TA 2	Unit
Motor voltage	24	24	V
Maximum load	150	120	N
Maximum speed at 24 V	40 to 45	33 to 44	mm/s
Motor speed at 24 V	6000	4000	RPM
Rod stroke	200	150	mm
Gear ratio	5:1	5:1	–
Typical current	2	1.2	A

The EMAs are driven by the fully integrated EV-VNH7070AS H-bridge drivers manufactured by STMicroelectronics. These drivers enable controlling in ranges up to 28 V, 15 A, and PWM up to 20 kHz. They are also equipped with various protection functions such as overvoltage protection, short-circuit protection, thermal fuse, current and power protection or inductive voltage diodes.

The block diagram also comprises three different power supplies used in the system and a conditioning circuit responsible for amplifying the force sensor signal and noise reduction.

3.2. Mechanical construction

The testing system's mechanical construction comprises a frame, linear guides, one or two EMAs, and brackets to attach the actuators and sensors. The frame is made of lightweight aluminium, and can be modified based on the actuator's specific dimension. The construction with one EMA is shown in Fig. 7.

The tested EMA is attached to the frame at the bottom, and its upper part is connected to the movable trolley through a force sensor. The trolley slides on guides in a linear motion and allows force-loading of the tested actuator, using either static weight or artificial load. The static weight is composed of metal blocks for scalable force loading in one direction. In order to achieve variable force loading in both directions, a secondary actuator can be attached.
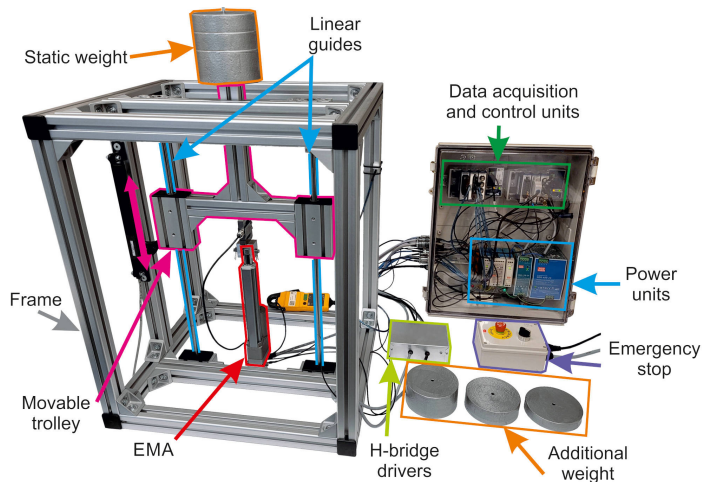
Fig. 7. Mechanical construction of the testing system with the TA 2 actuator.

4. Experimental Results

4.1. Jam detection

The algorithm for jam detection was verified in a series of experiments. The testing was performed for different working conditions, including various duty cycles, movement speeds, and loads. Conditions during experiments were determined as follows: $f_S = 2$ kHz, $f_P = 16$ kHz, $a = 3$, $N_{wp} = 38$ (see (1)) and the longest time of a commutation spike was measured as $T_{max} = 67.6$ ms, therefore $N_{wc} = 13520$ (see (2)). This period corresponds to the rod's movement at a rate of $v_{min} = 0.8$ mm/s, which is about 1.7% of the maximum speed. The fault detection thresholds are determined from the measurements conducted on the EMA without any load at the lowest speed. The span of values of commutation peaks and the averaged current in this measurement are minimal compared to all possible states during the nominal operation of EMA. Therefore, thresholds are established as 50% of these values to ensure acceptable margins. The resulting thresholds came out as $X_{pp} = 50$ mA and $X_a = 65$ mA.

The jam fault was simulated using a solid mechanical barrier in the path of the actuator rod. The rod impact into the barrier was either direct (hard stop) or gradual using a resilient insert (soft stop). The example of current change measured during the jam fault is depicted in Fig. 8. The figure illustrates the course of averaged and peak-to-peak signals that the algorithm uses for fault detection.

Two outcomes from the method testing are shown in Fig. 8. The experiment in Fig. 9a was performed with the duty cycle $D = 100\%$ and the evaluation time set to $T_o = 0.1$ s. The nominal operation can be seen at the beginning of the experiment. After about 500 ms the load is so high that the motor cannot move anymore, and the algorithm detects a fault which is highlighted in the frame called "Fault detection" (values 1 or 0). The detected state is evaluated after the set time has elapsed as a jam fault. This experiment shows the case of a hard stop at the full speed of the actuator. The raw data are fully overlapped by filtered data in this case, as explained in Section 2.1. Figure 9b shows a situation where the actuator was driven slowly ($D = 20\%$) to a soft stop. Oscillations between 3 to 4.5 seconds in the filtered signal demonstrate the deformation of resilient material before the jam.
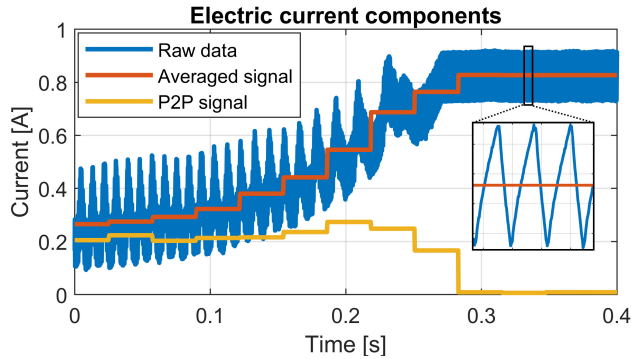
Fig. 8. Example of calculated components of electric current during the jam of an EMA.
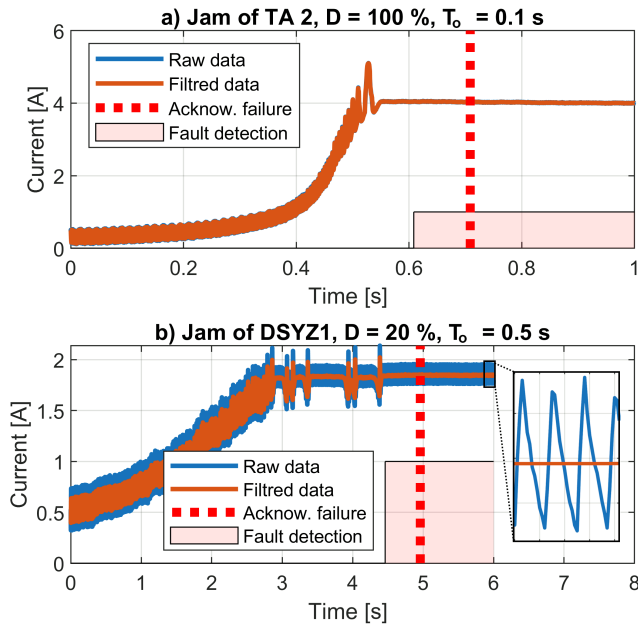

Fig. 9. Jam fault detection: a) hard stop, b) soft stop.

It can be seen from Fig. 9a and 9b that by setting a longer time to acknowledge the fault, false positive detection can be prevented.

Figure 9b also demonstrates that simple overcurrent current protection would be not sufficient. When the EMA is driven using low duty cycles, the averaged current is within the nominal range even when the actuator is jammed.

The proposed method was tested and evaluated using 35 records of nominal (no fault injected) operation and 34 records containing jam faults. Each test was performed under different operating conditions. The duration of the jam fault was higher than 500 ms in 31 records, two had jams shorter than 300 ms, and one had a jam fault between 300 and 500 ms. The confusion matrices in Fig. 10 summarise the ability of the presented method to detect faults.

	a) 0.5 s		b) 0.3 s		c) 0.1 s	
	Det. state: Nominal	Det. state: Fault	Det. state: Nominal	Det. state: Fault	Det. state: Nominal	Det. state: Fault
True state: Nominal	35	0	35	0	33	2
True state: Fault	3	31	2	32	0	34

Fig. 10. Confusion matrices for jam detection with different evaluation times:
a) 0.5 seconds, b) 0.3 seconds, c) 0.1 seconds.

The method uses three measured motor parameters that can vary for individual motors piece by piece. The effect of variability T_{max} and minimal of peak-to-peak and averaged current were tested. The experiments were performed for each of the tested parameters separately. Individual parameters were examined in the range of 5 to 195% of the correct measured value. The testing was conducted for a set of 32 nominal records and 32 records with jam faults. The set of records was selected to be always correctly evaluated at 100% of the tested parameter. All experiments were conducted for $T_o = 0.3$ s. The results from the experiments are shown in Fig. 11.
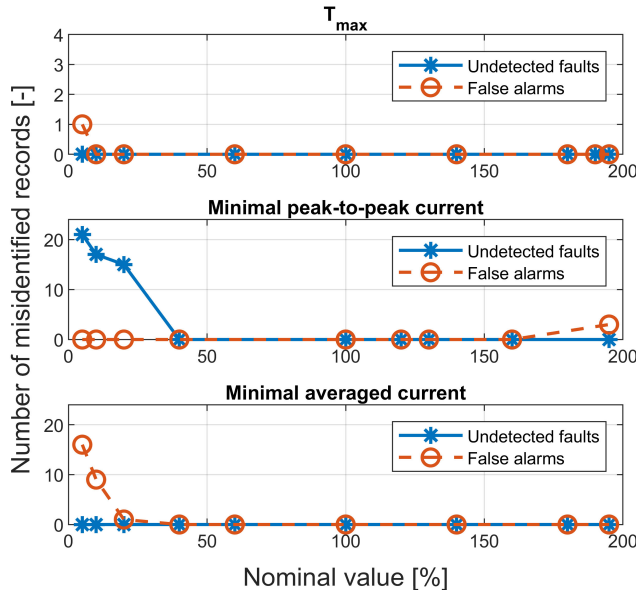

Fig. 11. Influence of input parameters on the jam detection method.

4.2. Winding short detection

The winding short detection method was tested during the DSZY1 actuator's faulty and nominal operation. During tests, the actuator was autonomously driven by a controller that moved the rod along predefined trajectories. The function generator produced a position set-point, which formed sinusoidal, triangular and rectangular motion profiles. The EMAs were exposed to loads 20%, 53%, 100%, and 120% of the nominal load for each motion profile during experiments. Two faults were injected by artificially shortening the two nearest turns of the rotor coil. In the case of Fault 1, two turns of the same coil were shorted, and in the case of Fault 2, two turns of different coils were shorted. The artificial faults are shown in Fig. 12.
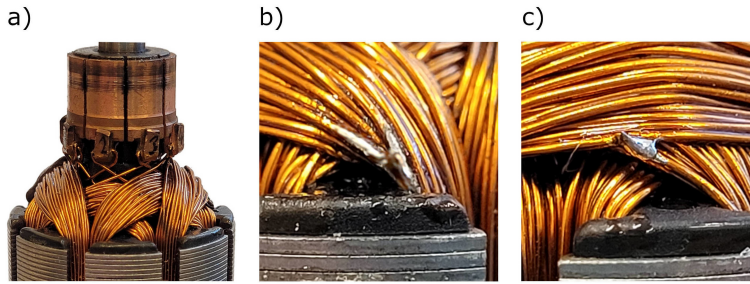
Fig. 12. Rotor winding – a) intact winding, b) detail of Fault 1, c) detail of Fault 2.

Conditions during the experiments were determined as follows: $v_{\max} = 6000$ RPM, $r = 10$ thus $T_d = 0.2$ s (see (5)), $f_S = 200$ kHz and $f_\Delta = 5$ Hz (see (6)). The following examples illustrate the function of the proposed method's data selection and spectrum analysis blocks.

An example of data selection is shown in Fig. 13. The sinusoidal motion profile, which includes various motor speeds, was applied during the experiment.
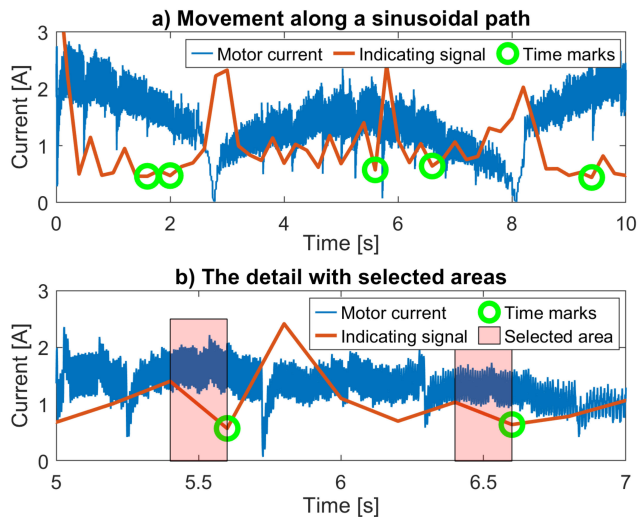

Fig. 13. Example of data selection based on the indicating signal.

Figure 13 shows time marks at the end of selected data segments. The amplitude of the indicating signal is multiplied by two for better visibility. Notice that the indicating signal is high after rapid changes in the current and low when the signal is uniform; selected areas were used for spectrum analysis.

An example of analysis with three different cases is depicted in Fig. 14. The "Low speed" case shows a situation where the frequency found in the required range is, in fact, the second harmonic commutation frequency. The algorithm therefore continuously checks whether the significant peak is at half the value of the found peak to detect the fundamental commutation frequency correctly.

Winding short detection is based on searching for the significant amplitude at twice f_M. Figure 14 shows the case of a winding short where the significant amplitude should be at frequency
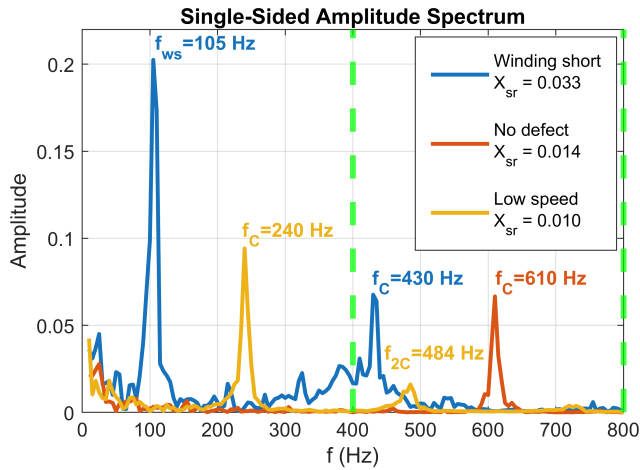
Fig. 14. The amplitude spectrum analysis where f_C are fundamental commutation frequencies, f_{2C} is the second harmonic of f_C and f_{ws} is a winding short fault. The area between dashed lines represents the required speed range (in this case 50-100%) for which the calculated X_{sr} thresholds are displayed. The X_{ws} threshold is defined as half of the f_C amplitude.

$f_{ws} = 2 \cdot f_C/N_C = 2 \cdot 430/8$, thus $f_{ws} = 107.5$ Hz. The peak at 105 Hz reveals the winding short. The threshold defining fault was set at amplitude as $X_{ws} = X(f_C/2)$. The height of f_{ws} is three times more than f_C, indicating the distinctive extent of the damage. The "No defect" case shows no significant peak lower than commutation frequency, which means no fault is present. The algorithm also excludes inappropriate data from analysis when the speed of the motor varies. Varying speed is exhibited by the low amplitude and a smeared peak of examined frequency. The measurements showed that a sharp peak during nominal operation is usually more than ten times higher than the mean value The threshold X_{sr} was therefore set to quintuple of the mean value. Thresholds are always calculated for each case individually, which can be seen in Fig. 14.

Three outcomes from the method testing are shown in Fig. 15. This example shows one period of rectangular, sinusoidal and triangular motion profiles.

Green, red or grey highlighted stripes are areas selected by the data selection algorithm. Figure 15a shows the output of the detection method during nominal operation. The rectangular motion profile, which includes areas where the actuator holds the target position, was applied during the experiment. These areas are not suitable for fault detection, and therefore they have been automatically excluded from the processing. The relevant areas are evaluated as nominal. Figure 15b and 15c shows examples of sinusoidal and triangular movements with winding short faults. After three positive fault indications, the winding short failures are acknowledged in both cases.

The fault detection ability of the proposed method was evaluated in a set of experiments. The set consisted of 24 nominal records, 12 with Fault 1 and 12 with Fault 2. Figure 16 summarises the ability to detect faults after a certain time.

An essential input parameter of the method is the maximum RPM. This parameter may vary slightly for individual motors, and therefore the influence of RPM has been further investigated. The effect was tested on a set of 24 nominal records and 24 records containing winding short faults. Each of the records was 44 seconds long. The parameter was placed between 70 and 130% of the correct value during testing. The result of the experiment is shown in Fig. 17.
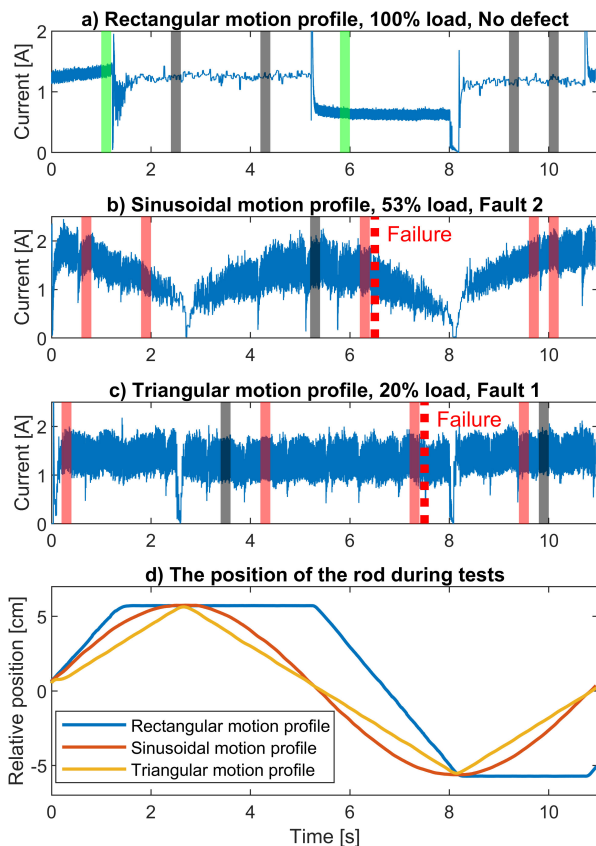
Fig. 15. Example of outcomes from the winding short detection algorithm (a, b, c) and the position of actuator rod recorded during these experiments (d). Highlighted stripes represent the data blocks selected for spectrum analysis, and their colour indicates results: green – no fault detected, red – a winding short detected, grey – data excluded from fault detection analysis (low or changing motor speed), a red dashed stripe – fault confirmed.

	a) 8 s		b) 11 s		c) 14 s	
	Det. state: Nominal	Det. state: Fault	Det. state: Nominal	Det. state: Fault	Det. state: Nominal	Det. state: Fault
True state: Nominal	24	0	24	0	24	0
True state: Fault	8	16	3	21	0	24

Fig. 16. Confusion matrices with different record lengths used for evaluation of fault detection:
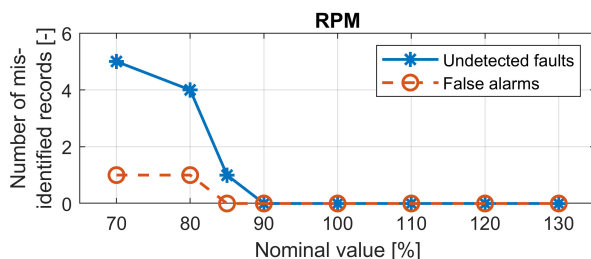a) 8 seconds, b) 11 seconds, c) 14 seconds.

Fig. 17. Influence of input parameter on the winding short detection method.

5. Discussion

The performed experiments point out to some beneficial properties of the presented methods. The advantage of both presented methods is that they use only basic electromechanical properties of the actuator and the electric current measurement. For comparison, other jam detecting methods require additional sensors to measure parameters such as temperature, vibration or position [15] or statistical approaches utilising learning [7].

In the case of winding shorts, there are some methods for faults detection in EMAs with *brushless DC* (BLDC) motors [16]. Due to the different electrical excitation of the winding, the manifestation of faults is entirely dissimilar, and these methods cannot be used for EMAs with brushed DC motors. For a brushed DC motor, there are some *hidden Markov model* (HMM)-based methods [17]. Unlike the proposed methods, these techniques use a supervised learning approach, which is a significant disadvantage preventing their use in industry.

The proposed methods are also able to deal with the dynamic behaviour of EMA operation. The jam detection method uses dynamic changes during operation to evaluate the movement of EMA, while the winding short fault detection method utilises a novel approach to distinguish in which sections of the signal the analysis should be performed. In contrast to other techniques that utilise additional sensors or procedures, such as various order tracking or machine learning methods, the proposed approach does not require supplementary information sources and complex implementations.It can therefore be easily implemented in embedded devices such as generic 200 MHz microcontrollers or directly into control units typically equipped with current sensing [5].

The detection speed is different for each method. In the case of jam detection, the time to detect a fault is given by the evaluation time, which was never longer than half a second during the experiments. In the case of winding short detection, the time of fault detection depends on the extent of the failure, chosen thresholds, and the most on the actuator operation conditions. The time to detect a fault can vary in the range of several to tens of seconds. Even though the fault may not be confirmed immediately, it is possible to inspect its development by monitoring the defect amplitude in the spectrum.

Both methods are equipped with fault evaluation procedures that help avoid incorrect classification. In the case of the jam detection method, the evaluation time should be set individually according to the required detection sensitivity. The fault evaluation procedure of the winding short detection method ensures that the method classifies nominal records correctly. It delays the fault confirmation but also increases the detection accuracy.

The proposed methods were also tested for sensitivity to the variability of input parameters. The winding short detection method is more sensitive to maximal speed parameters, which may cause false alarms when the motor has higher RPM than expected. However, the loaded actuator tends to operate slower, so this limitation is not crucial.

6. Conclusions

This article introduces two data-based fault detection methods for *electromechanical actuators* (EMAs) with a brushed DC motor. Both methods are based on an analysis of motor current intensity.

The first method for jam detection is based on monitoring commutation oscillations that indicate the motor's movement. The detected oscillations are compared with the average current utilising electromechanical parameters of the EMA determined during nominal operation. The relation between these parameters allows identifying whether the actuator is jammed. Unlike

conventional overcurrent protection, the proposed procedure provides jam fault detection even during operation when the power or force of the actuator is limited.

The second method detects winding short faults. The operation of an EMA tends to have the rapid speed or direction changes based on the mode of operation. The measured current is first examined to find time periods suitable for reliable fault detection. The proposed algorithm uses a novel data selection procedure that utilises the kurtosis and coefficient of variation to estimate the motor's stable operation. Selected signal sections are processed using spectrum analysis to find frequencies that indicate a winding short fault. This approach allows the detection of the fault and monitoring of development and the extent of the fault by comparing the measured amplitudes.

Both methods were tested using a series of experiments, and their ability to detect defects was evaluated. The experiments proved that proposed methods can work under various modes of operations, including rapid changes in speed or direction of motor rotation, variable loads, or different movement regimes and detect faults successfully. In addition, the robustness of both methods was verified via a variety of experiments that tested the sensitivity to input parameters. The advantage of the presented methods is that they only require knowledge of the EMA's basic electromechanical properties, such as maximum and minimum motor speeds and commutator arrangement. Also, they employ the measurement of only one quantity, motor current intensity, which is accessible on the motor driver. Thanks to the non-intrusive approach and low computational complexity, the proposed methods are easy to implement in industrial applications utilising EMAs.

The research results and benefits of the proposed approach can be summarized as follows:
- The proposed methods utilise only the current measurement and basic electromechanical properties of actuators.
- They do not require any additional sensors, sources of information or complex data processing methods to work under varying operating conditions.
- They are easy to implement because they do not need interventions into the actuator, thanks to a non-intrusive approach.
- They utilise techniques to reduce computational complexity, and therefore diagnostics can be performed at the level of the control power unit.

Future work will be devoted to further development of non-intrusive approaches. Measurement and processing of electrical voltage in combination with the current can significantly expand the number of detectable faults. In addition, data measured during operation can be compared with historical data, which will benefit predictive systems that monitor equipment service life.

Acknowledgements

References

[1] Chirico, I., Anthony, J., & Kolodziej, J. R. (2014). A Data-Driven Methodology for Fault Detection in Electromechanical Actuators. *Journal of Dynamic Systems, Measurement, and Control*, *136*(4). https://doi.org/10.1115/1.4026835

[2] Arriola, D., & Thielecke, F. (2017). Model-based design and experimental verification of a monitoring concept for an active-active electromechanical aileron actuation system. *Mechanical Systems and Signal Processing*, *94*, 322–345. https://doi.org/10.1016/j.ymssp.2017.02.039

[3] Di Rito, G., Schettini, F., & Galatolo, R. (2018). Model-Based Prognostic Health-Management Algorithms for the Freeplay Identification in Electromechanical Flight Control Actuators. *2018 5th IEEE International Workshop on Metrology for AeroSpace*, 340–345. https://doi.org/10.1109/MetroAeroSpace.2018.8453552

[4] Balaban, E., Bansal, P., & Stoelting, P. (2009). A diagnostic approach for electro-mechanical actuators in aerospace systems. *2009 IEEE Aerospace conference*, *2009*. https://doi.org/10.1109/AERO.2009.4839661

[5] Ruiz-Carcel, C., & Starr, A. (2018). Data-Based Detection and Diagnosis of Faults in Linear Actuators. *IEEE Transactions on Instrumentation and Measurement*, *67*(9), 2035–2047. https://doi.org/10.1109/tim.2018.2814067

[6] Ismail, M. A. A., Balaban, E., & Spangenberg, H. (2016). Fault detection and classification for flight control electromechanical actuators. *2016 IEEE Aerospace Conference*, 1–10. https://doi.org/10.1109/AERO.2016.7500784

[7] Mazzoleni, M., Previdi, F., Scandella, M., & Pispola, G. (2019). Experimental Development of a Health Monitoring Method for Electro-Mechanical Actuators of Flight Control Primary Surfaces in More Electric Aircrafts. *IEEE Access*, *7*, 153618–153634. https://doi.org/10.1109/ACCESS.2019.2948781

[8] Wang, C., Tao, L., Ding, Y., Lu, C., & Ma, J. (2022). An adversarial model for electromechanical actuator fault diagnosis under nonideal data conditions. *Neural Computing and Applications*, *34*(8), 5883–5904. https://doi.org/10.1007/s00521-021-06732-x

[9] Zhao, D., Cheng, W., Gao, R. X., Yan, R., & Wang, P. (2020). Generalized Vold–Kalman Filtering for Nonstationary Compound Faults Feature Extraction of Bearing and Gear. *IEEE Transactions on Instrumentation and Measurement*, *69*(2), 401–410. https://doi.org/10.1109/TIM.2019.2903700

[10] Yuyan, C., Jian, W., Rong, X., & Xinmin, W. (2015). Fault tree analysis of electro-mechanical actuators. *2015 34th Chinese Control Conference (CCC)*, 6392–6396. https://doi.org/10.1109/ChiCC.2015.7260646

[11] Stone, G. C. (2004). *Electrical insulation for rotating machines: design, evaluation, aging, testing, and repair*. Wiley-Interscience

[12] Westfall, P. H. (2014). Kurtosis as Peakedness, 1905 – 2014.R.I.P. *The American Statistician*, *68*(3), 191–195. https://doi.org/10.1080/00031305.2014.917055

[13] Lee, S. B., Shin, J., Park, Y., Kim, H., & Kim, J. (2021). Reliable Flux-Based Detection of Induction Motor Rotor Faults from the Fifth Rotor Rotational Frequency Sideband. *IEEE Transactions on Industrial Electronics*, *68*(9), 7874–7883. https://doi.org/10.1109/TIE.2020.3016241

[14] Park, Y., Choi, H., Shin, J., Park, J., Lee, S. B., & Jo, H. (2020). Airgap Flux Based Detection and Classification of Induction Motor Rotor and Load Defects During the Starting Transient. *IEEE Transactions on Industrial Electronics*, *67*(12), 10075–10084. https://doi.org/10.1109/TIE.2019.2962470

[15] Hussain, Y., Burrow, S., Henson, L., & Keogh, P. (2020). A Review of Techniques to Mitigate Jamming in Electromechanical Actuators for Safety Critical Applications. *International Journal of Prognostics and Health Management*, *9*. https://doi.org/10.36001/ijphm.2018.v9i3.2749

[16] De Martin, A., Jacazio, G., & Vachtsevanos, G. (2017). Windings Fault Detection and Prognosis in Electro-Mechanical Flight Control Actuators Operating in Active-Active Configuration. *International Journal of Prognostics and Health Management*, *8*. https://doi.org/10.36001/ijphm.2017.v8i2.2633

[17] S Zhang, J., Zhan, W., & Ehsani, M. (2018). On-line diagnosis of inter-turn short circuit fault for DC brushed motor. *ISA Transactions*, *77*, 179–187. https://doi.org/10.1016/j.isatra.2018.03.029

Ondřej Hanuš received his M.Sc. degree in electrical engineering from Czech Technical University in Prague in 2014, where he is currently pursuing a Ph.D. degree. He currently works with the Department of Measurement as a Research Assistant. He has experience in non-destructive testing, fault detection and diagnosis, detection of degradations and electric energy consumption-based monitoring. His field of research is the measurement and monitoring of energy consumption in aviation.

Radislav Smid (IEEE member) is currently the Head of the Laboratory for Diagnostics and Nondestructive Testing and a Full Professor with the Department of Measurement, Faculty of Electrical Engineering, Cech Technical University in Prague. His major research interests include instrumentation and signal processing for non-destructive testing, SHM, MCM, and PHM.